Aleksandar Sedmak[1*], *Katarina Čolić*[2], *Simon Sedmak*[2]

STRUCTURAL INTEGRITY AND LIFE OF HIP IMPLANTS: REVIEW OF CASE STUDIES

INTEGRITET I VEK VEŠTAČKIH KUKOVA: PREGLED STUDIJE SLUČAJEVA

Originalni naučni rad / Original scientific paper
Rad primljen / Paper received: 1.12.2025
https://doi.org/10.69644/ivk-2025-03-0509

Adresa autora / Author's address:
[1)] University of Belgrade, Faculty of Mechanical Engineering, Belgrade, Serbia A. Sedmak https://orcid.org/0000-0002-5438-1895 ; *email: aleksandarsedmak@gmail.com
[2)] Innovation Centre of the Faculty of Mechanical Engineering, Belgrade, Serbia K. Čolić https://orcid.org/0000-0002-0227-0026
S. Sedmak https://orcid.org/0000-0002-2674-541X

Keywords
- hip implants
- biomaterials
- finite element method
- fatigue crack growth

Ključne reči
- veštački kuk
- biomaterijali
- metoda konačnih elemenata
- rast zamorne prsline

Abstract

Hip implants are nowadays typically high-quality and reliable components which rarely fail. Nevertheless, they still sometimes do, due to static, impact or amplitude loading, under hostile environment such as our bodies. Therefore, we still have to analyse factors that may affect both hip implant integrity and life, such as body weight, implant geometry and material. In this paper, a review of recent investigation of hip implant fracture and fatigue behaviour is presented with focus on the effects of body weight, implant geometry and material. It is shown that body weight plays an important role, especially for fatigue life, since the relation between remaining life and stress (proportional to weight) is exponential (typically m = 3 in Paris equation). Regarding implant geometry, it is demonstrated that the main issue is stress analysis. In the case of modular (full cross-section) implants, stress state is more favourable than in the case of implant with holes for fine adjustment according to patient bone configuration. It is also shown that stress level in this case can be surprisingly high, especially with younger, active patients. Finally, the interaction between influencing factors should be taken into account, being a relatively simple task when numerical methods are used.

Izvod

Veštački kukovi su danas tipično kvalitetne i pouzdane komponente koje retko otkazuju. Ipak, ponekad se to dešava, zbog statičkog, udarnog ili amplitudnog opterećenja, u neprijateljskom okruženju kao što su naša tela. Stoga, i dalje trebamo analizirati faktore koji mogu uticati i na integritet i na vek trajanja implantata kuka, kao što su telesna težina, geometrija implantata i materijal. U ovom radu, dat je pregled nedavnih istraživanja o lomu i ponašanju veštačkog kuka pri zamoru, sa fokusom na efekte telesne težine, geometrije implantata i materijala. Pokazano je da telesna težina igra važnu ulogu, posebno za vek trajanja usled zamora, jer je odnos između preostalog veka i napona (proporcionalan težini) eksponencijalan (tipično m = 3 u Parisovoj jednačini). Što se tiče geometrije implantata, pokazano je da je glavno pitanje analiza napona. U slučaju modularnih (punog poprečnog preseka) implantata, stanje napona je povoljnije nego u slučaju implantata sa rupama za fino podešavanje prema konfiguraciji kostiju pacijenta. Takođe je pokazano da nivo napona u ovom slučaju može biti iznenađujuće visok, posebno kod mlađih, aktivnih pacijenata. Konačno, treba uzeti u obzir i interakciju između uticajnih faktora, što je relativno jednostavan zadatak kada se koriste numeričke metode.

INTRODUCTION

Hip implants should serve for a lifetime of a patient, but in reality there are still a number of cases of failure, mainly due to fatigue, /1-6/. Failures of hip implant of 13 patients are analysed in /1/, pointing out that the femoral neck is broken in 4 cases, the stem in 5 cases, 1 inlay failure, 2 cup failures and 1 conus dislocation. The focus of this analysis is on body mass index (BMI) mean value 31.42±5.29 kg/m^2. It is concluded that failures do not seem to correlate with participation in sports or BMI, /1/. In /2/ a complete fracture of the modular femoral neck is presented and analysed as a case study.

Fracture of Co-Cr modular neck in total hip arthroplasty is presented in /3/. It is noticed that Ti alloy breakage at the femoral neck became a concern, so the cobalt-chrome (Co-Cr) alloy is used instead. However, a few cases of Co-Cr modular neck breakage are also reported and two are described in /3/. Risk factors, such as long varus type of modular neck, overweight and/or high demanding physical activity, are identified.

Similar to the previous research, authors of an extensive study /4/, have analysed and identified factors causing neck fracture associated with commonly used bimodular THA design. Major purposes of this study are to define the proportion of patients who experience fracture of the stem modular femoral neck; and to determine factors associated with neck fracture. It is also mentioned that Ti alloy necks are replaced by CoCr alloy neck. Anyhow, this type of CoCr neck is recalled in 2015 due to even higher fracture rates.

In paper /5/ a large database with mechanical failure of a single uncemented modular femoral component is evaluated and used to calculate the fracture rate. There were 113 recorded cases with fracture at the modular junction, providing fracture rate of 0.3 % (113/37,600), or less if only implants without signs of improper use are taken into account - 0.11 % (41/37,600). In 79 % (89/113) of cases either a lateralised (high offset) neck segment, an extralong head, or both

are used. Thus, it is concluded that implant failure at the modular junction is associated with patient- and implant-specific risk factors as well as technical errors during implantation.

Premature failure of a total hip prosthesis implanted in an active patient is analysed in /6/. The prosthesis replaced a fractured stem that was extracted from a 46 year old male patient, 75 kg weight after 5 years of exploitation. It was shown that the crack originated on the anterolateral corner section of the stem due to stress concentration and any discontinuity or defect in this location.

Narrative review is made on the causes of hip failure, including the prevalence, diagnosis, risk factors, and treatment options. As the result, periprosthetic joint infection, dislocation, malalignment/malposition, iliopsoas impingement, and other causes of pain after THA are identified.

Three different metallic materials, namely cobalt chromium molybdenum alloy, stainless steel 316L (SS 316L), and titanium alloy (Ti6Al4V) are evaluated for application in metal-on-metal bearing of total hip implant in terms of contact pressure, i.e., wear resistance, /8/. A silico model based on finite element simulation is considered to predict contact pressure of metal-on-metal bearings under normal walking conditions. It is found that the use of Ti6Al4V-on-Ti6Al4V is superior in its ability to reduce contact pressure by more than 35 % compared to the other studied metal-on-metal couple bearings.

In /9/ loosening of model cemented joint replacement specimens is examined under cyclic loading and the fatigue strength of bone/cement interface is evaluated, suggesting that the fatigue strength of the bone/cement interface in cemented total joint replacements can be estimated from simple quasi-static shear tests.

The clinical use of 3D printing in orthopaedics was critically reviewed, focusing on cementless acetabular components used in total hip arthroplasty, /10/. Whilst early clinical outcomes related to 3D printed cups have been promising, the long-term clinical outcomes are still needed to enable smooth transition to 3D printing technology.

In paper /11/ a premature fracture of a collared, polished and cemented hip stem, made of cast stainless steel, was investigated by radiographic fracture analysis, material characterisation and S-N fatigue tests. Also, numerical simulation of the stem under the ISO 7206-4 standard test and under a well stabilised arthroplasty hypothesis is performed to predict failure. It is shown that the use of the 'as cast' austenitic stainless steel ASTM F 745 is not suitable for implants that have potential for fatigue failure.

Dual modular Ti alloy stems, enabling better control of the femoral offset, leg length, and hip stability are systematically reviewed in respect to modular neck fracture. It is shown that dual modular stems have no clinical benefits for patients, since they exhibit worse results than monolithic stems.

Two fractures of a modular, tapered and distally fixed, uncemented titanium revision hip stems are presented, /13/. A failure analysis reveals fatigue cracks growth in the mid - stem Co-Cr modular junction ending in corrosion fatigue failure. No material defects or stress risers are found, so it seems that the diameter of the midstem modular junction is undersized for use in heavy and active patients, /13/.

Fatigue failures of different hip profiles are analysed and compared for various combinations of shapes, profiles and materials, /14/. Circular, oval, elliptical, and trapezoidal shaped stems, each with 3 profiles, are analysed, with 4 different material combinations based on Ti6Al4V, CoCr alloy and UHMWPE, 48 combinations in total. A numerical simulation is performed by ANSYS 2022 R1 with ISO 7206-4 and ASTM F2996-13 standards used for boundary conditions. Profile 2 of the trapezoidal-shaped hip implant with a Ti6Al4V stem exhibited superior results both under static and fatigue loading conditions, /14/.

Another failure analysis of femoral components identified several factors, including implant material, type and positioning, cementing technique, and loading /15/.

Obviously, as shown by the literature review, there are high demands for hip implants to be fulfilled to sustain mechanical loads, both static and dynamic, and an environmental challenge of the human body. In order to meet these high demands, implant geometry and material are crucial. Titanium and Co-Cr alloys are most frequently used, but both known for their sensitivity to cracks or notches. Although not in focus here, one should notice that Ti alloys have another important advantage since their modulus of elasticity is significantly closer to that of a natural bone, so the shielding effect is much less pronounced, as explained in /16/. Consequently, the hip implants still must be analysed to assess their structural integrity and life.

To complete the introduction, let us state that the authors of this paper have a long time experience in analysing different aspects of structural integrity and life of different hip implant, including different materials and geometries, /17-27/. Here, a review of these papers is presented in a form of case studies, with a critical analysis and discussion of the results. Brittle fracture and fatigue are in the focus of these researches performed on two materials mostly used for hip implants - CoCr based alloys and Ti6Al4V or similar Ti alloys. Two different geometries were analysed, full cross-section and with two openings.

Papers /17-25/ deal with full cross-section hip implants, with a focus on necking area, as a critical one under both static and dynamic/fatigue loading, including also corrosion effects, /22-24/. Hip implants with two openings are analysed in papers /25-29/, with a focus on high stresses in remaining area where openings are positioned.

The DIC and FEM are used to get precise stress state under static loading, while xFEM (and FEM SMART) are used to evaluate fatigue life of a cracked implant. These two numerical methods for fatigue crack growth (FCG) simulation are described in a couple of review papers, /30-33/.

Experimental research is performed in accordance with the ISO 7206-4 standard /27/ for static loading. Results confirm relatively high sensitivity of both materials to crack growth, with somewhat better resistance to crack initiation. In respect to fatigue crack growth, the major problem turns out to be how to determine material properties (C and m in Paris law), especially if corrosion is taken into account.

Three case studies are presented here. The first one, standard/common analysis of CoCr full cross-section hip implant, the second is reverse engineering of Ti6Al4V (ELI) 'full' cross-section hip implant and the third, Ti-6Al-4V hip implant with holes.

CASE STUDY 1 - STANDARD/COMMON ANALYSIS OF CoCr FULL CROSS-SECTION HIP IMPLANT

In /17/, CoCr multiphase alloy is analysed with an attempt to determine the final stretch zone width as a fracture parameter. It is shown that critical J integral value can be obtained from J-R curve, corresponding well to the average stretch zone width.

In addition, finite element analysis of the implant for partial hip arthroplasty is performed, /17, 18/, both for static and dynamic loading, using 3-dimensional C3D8R and C3D10 elements. For static loading of the femoral component the forces ranged from 3.85 to 5.95 kN applied areas 442 and 377 mm^2. As presented in /17/, the maximal von Mises stress, located at the hip neck, was in range of 254-551 MPa, Fig. 1.

For crack propagation simulation, extended finite element method (XFEM) is used. Initial crack is positioned at the location of maximum stress. K_I, K_{II} and K_{III} are evaluated, indicating dominance of K_I. For crack growth from 0.5 to 8 mm (model 1/load 3845 N), almost 30,000 cycles are needed without going into unstable crack growth, whereas significantly lower number of cycles (644) are needed for crack growth from 0.25 to 3.5 mm (model 2/load 5964 N).

Results presented in /17, 18/ indicate low number of cycles to failure, i.e., high sensitivity of CoCr alloy to fatigue crack growth.

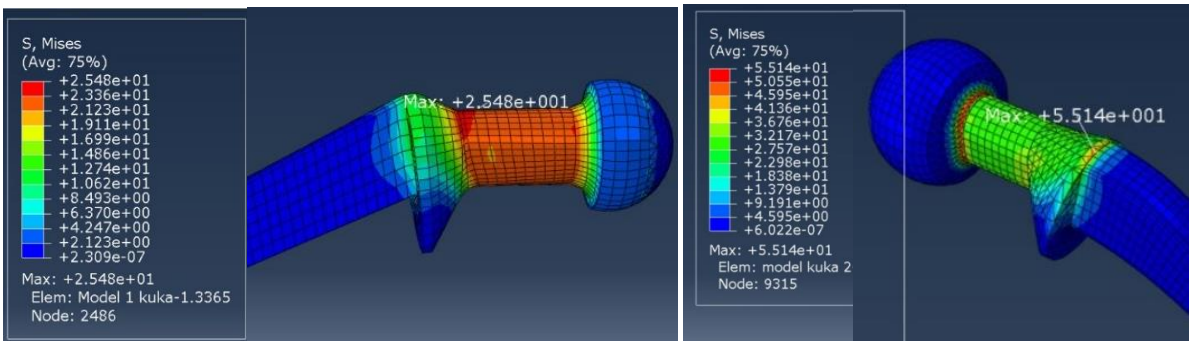

Figure 1. Stress distributions for: a) force of 3850 N, surface area 442 mm^2; b) force of 5985 N, surface area 377 mm^2.

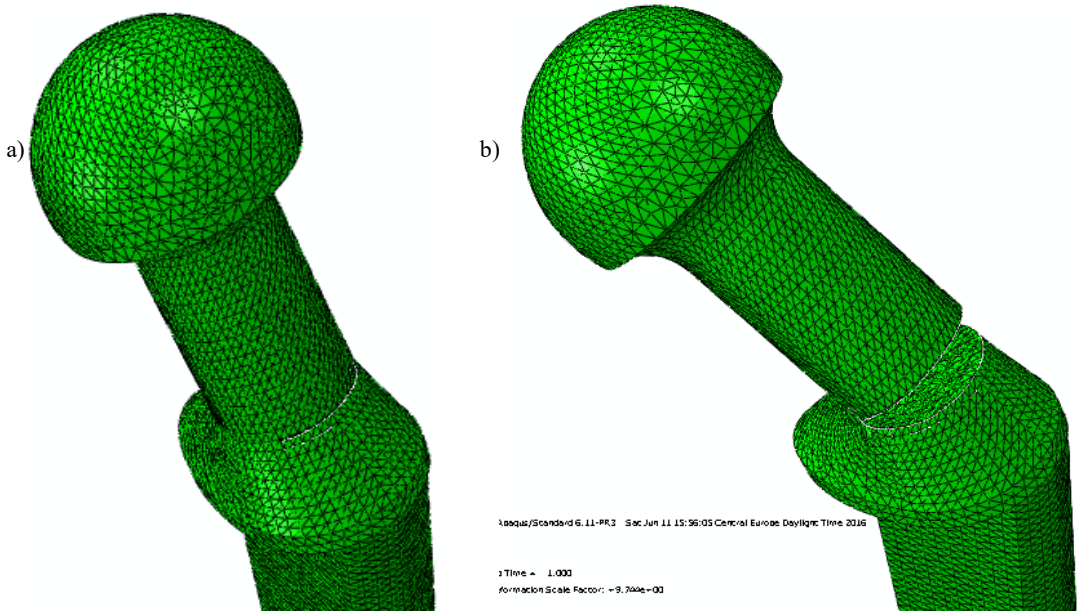

Figure 2. a) Model 1 crack 0.5 mm; b) model 1 crack 8 mm.

CASE STUDY 2 - Ti6Al4V (ELI) FULL CROSS-SECTION TOTAL HIP IMPLANT

Papers /19-22/ analyse the total hip replacement, made by precision casting of Ti6Al4V ELI (Extra Low Interstitials) alloy. To generate a geometrical model of hip implant, the 3D scanner is used and an obtained point cloud (PC), then exploited for reverse engineering to a CAD model. The neck thickness of implant is the focus of this analysis, since it affects the angle of movement of the joint and hip implant structural integrity. Reducing the thickness of the neck section results in higher movement of the joint but inversely affects its structural integrity. The 3D scanned implant has a neck thickness of 14.6 mm, and data from literature suggest that the best movement angle is for 9 mm thickness of the implant. To redesign the available implant, five different models with neck thickness between 9 and 14.6 mm are made, Table 1.

Table 1. Total number of finite elements and nodes.

Neck thickness (mm)	Total number of nodes	Number of elements
14.6	494613	343517
13.2	497589	343019
11.8	507746	350101
10.4	512094	353006
9	515202	354974

In paper /20/, reverse engineering is used to redesign a hip implant produced by precision casting, using Ti6Al4V extra low interstitials (ELI) alloy. As the most critical part, the hip neck has been in the focus of this analysis, keeping in mind that the lower is the thickness, the higher is the movement of the joint, but affecting its structural integrity at the same time.

Applied load, corresponding to stumbling is 8.7 times the body weight of a patient of 90 kg, defined as a concentrated force acting on the implant head, Fig. 3, whereas material properties used in this analysis are: $R_{p0.2}$ = 881 MPa, R_m = 971 MPa, modulus of elasticity is set to 120 GPa, the Poisson coefficient is 0.3 and fracture toughness K_{Ic} = 2100 MPa√mm.

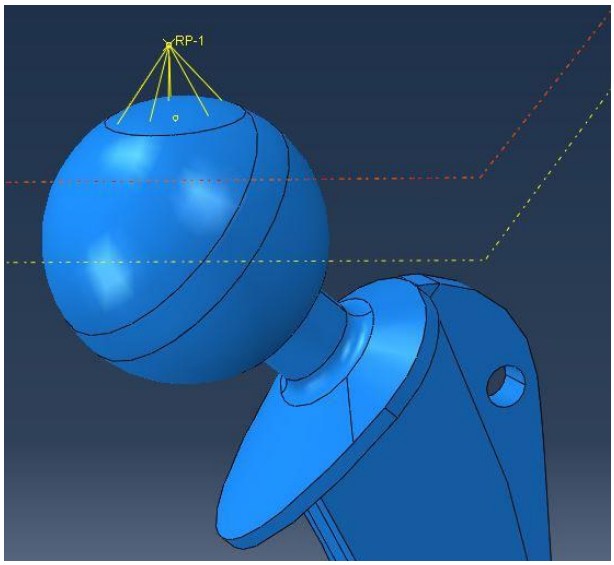

Figure 3. Loading in the model, defined as a concentrated force in a reference point

Additional four numerical models were made to evaluate maximum stress concentration at the front and back side of the neck with different thicknesses, i.e. 13.2, 11.8, 10.4 and 9 mm. The maximum stresses changed from 52 and 81 MPa (thickness 14.6 mm), to 89 and 114 MPa (neck thickness 13.2 mm), 102 and 123 MPa (11.8 mm), 125 and 150 MPa (10.4 mm), 179 and 202 MPa (9 mm). The last one is shown in Fig. 4 as an illustration of stress distribution. Area of stress concentration, on the model with lowest neck thickness, is much thicker vertically and narrower horizontally (more compact), compared to the previous numerical model. As the optimal model, neck thickness 10.4 mm was chosen, since stress values with neck thickness were unacceptable in presence of cracks.

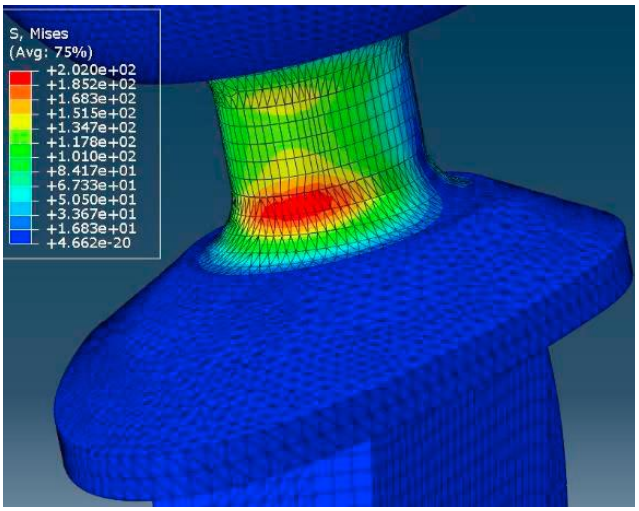

Figure 4. 9 mm neck as an illustration /20/

Further analysis included amplitude loading 3 kN, according to recommended values for normal walking load on hip joint for a person of 90 kg of mass /20/. Normal walking condition is the most suitable for numerical simulation of dynamic loading for regular multiyear exploitation of the total hip replacement implant. Coefficients for Paris equation were taken from ANSYS database, n=2.2, C=6.72e-13. Initial crack length was set at 1 mm and placed in the area of the highest stress, between implant neck and collar, Fig. 5. Remaining life for two models, one with neck thickness 14.6 mm, and the other one with 9 mm, are shown in Fig. 6.

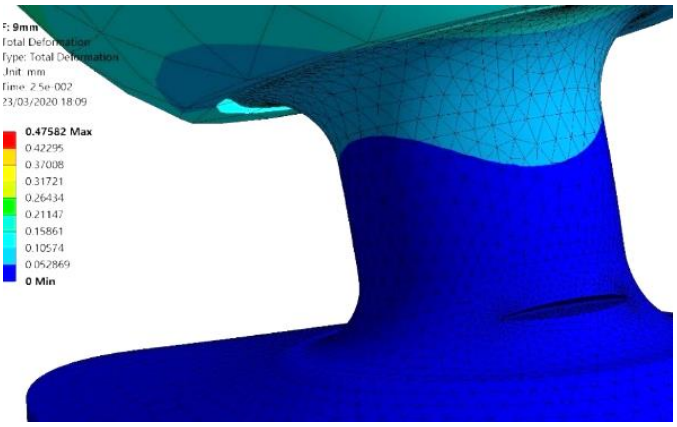

Figure 5. Crack opening displacement

a)

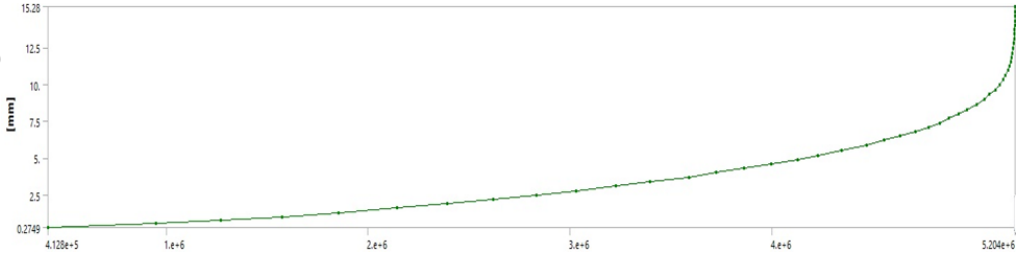

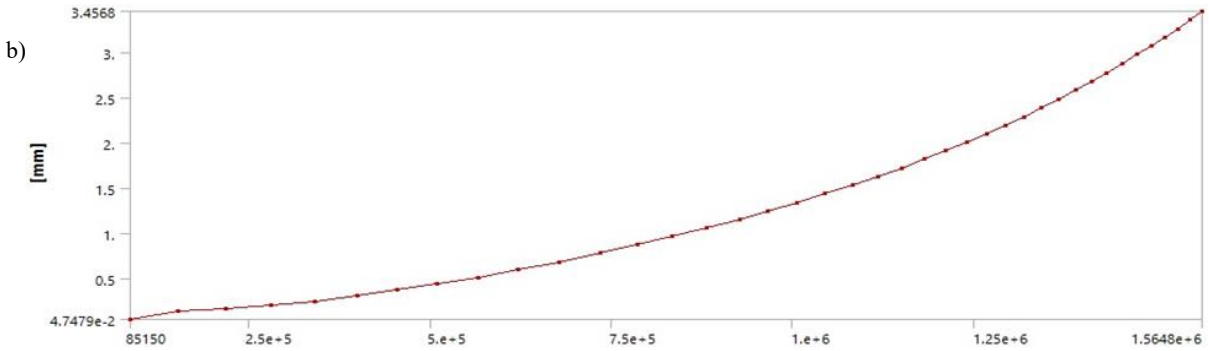

Figure 6. Crack length vs. number of cycles for: a) 14.6 mm neck; b) 9 mm neck.

As one can see from Fig. 6, hip implant with 14.6 mm neck thickness can withstand more than 5 million cycles, whereas the implant with 9 mm neck thickness fails at just 3.45 mm after 1.5 million cycles.

Similar to the previous two papers, numerical models are created in ABAQUS and ANSYS software packages, /21/, to determine stress/strain distribution, number of cycles to failure and stress intensity factors, for two hip implant full cross-section (with different neck diameters, 9 and 14.6 mm). This recalculation is performed for the loading due to patient weight 90 kg, to provide additional results in a form of the failure assessment diagram, assuming 1 mm initial crack length. As expected, the implant with the largest diameter provides safe point in FAD, while the smallest diameter shifts the point close to the limit curve.

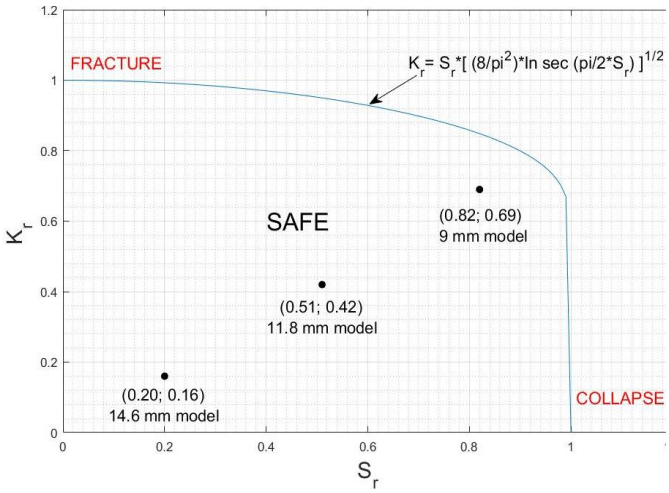

Figure 7. Failure assessment diagram for three hip joint models.

In /22/ fatigue crack growth in hip implant is analysed using the extended finite element method, as provided by ABAQUS® and Morfeo/crack, from initial until critical crack length. Initial crack dimensions are assumed according to the experience with failures of hip implants, whereas the final critical value is estimated using data for fracture toughness obtained by experimental testing of hip implant made of Ti6Al4V alloy. Results for the equivalent stress intensity factor and number of cycles in each of 40 steps of fatigue crack growth are presented and analysed, indicating the point of unstable crack growth, and are shown in Table 2.

The behaviour of the biomaterial of the stem artificial hip in the presence of a fatigue crack is first of all numerically simulated with an average working force of 2 kN, corresponding to slow walking, as explained in /5, 6/, producing amplitude stress $\Delta\sigma$ = 11.4 MPa.

Table 2. Results for fatigue crack growth parameters.

Ti-6Al-4V	Fatigue threshold ΔK_{th} (MPa·m$^{1/2}$)	Coefficient C	Exponent m
Sample 1	4.5	$1.54 \cdot 10^{-12}$	2.15
Sample 2	4.8	$3.70 \cdot 10^{-13}$	2.31
Sample 3	4.7	$1.05 \cdot 10^{-13}$	2.32

Figure 8. Geometry of real hip implant and different stem types

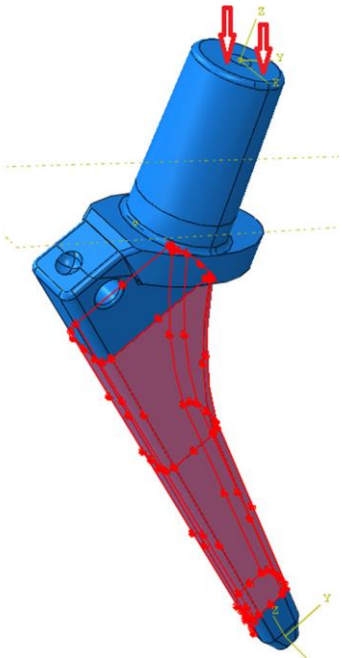

Figure 9. Numerical model with loads and boundary conditions.

Crack appearance and von Mises stress distribution are shown for the step 10 in Fig. 10, and for the final, 40th step, in Fig. 11. The initial numerically determined value of the stress intensity factor for the implant stem of Ti6Al4V with the assumed initial crack of 0.5 mm is 244 MPa√mm. By simulating crack growth in the biomaterial, that is, on the surface of the implant, the values of stress intensity factors increase, so that at the time the implant has failed completely, they reach values of 5017 MPa√mm.

a)

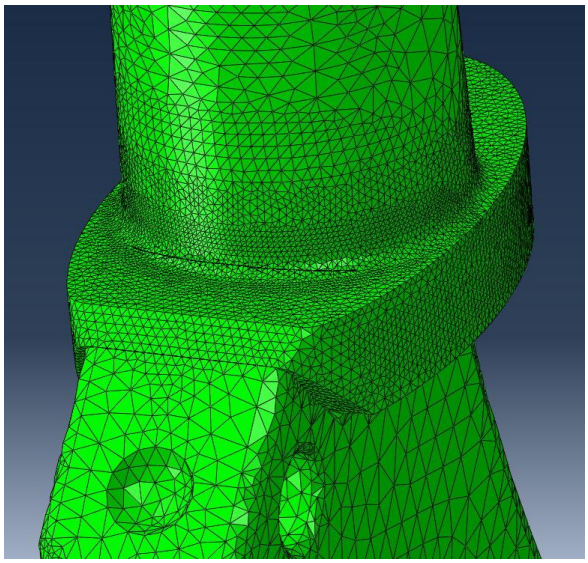

b)

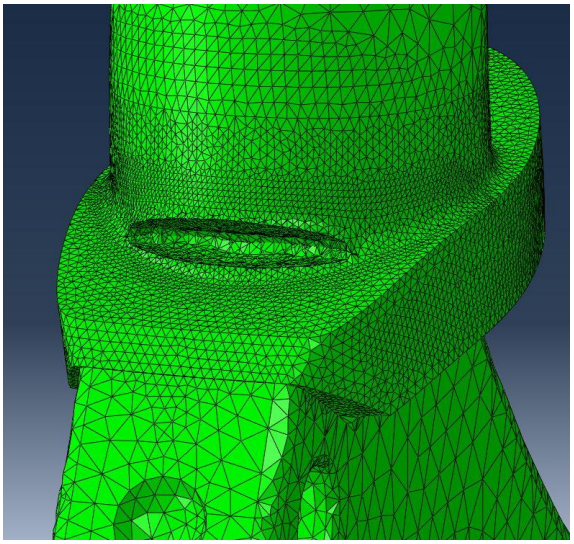

Figure 10. a) crack tip after step 10; b) crack growth over the entire length of the prosthesis.

The maximum value of K_I vs. crack length is shown in Fig. 12, whereas the crack length vs. number of cycles is shown in Fig. 13, indicating that the failure of implant stem will occur after 40 steps of crack growth, since both K_I and crack length start to grow in unstable manner. The corresponding number of cycles is 80,022,270.

The calculation number of walking cycles during the implantation period of the prosthesis that is needed to cause fracture due to cracks in the biomaterial is shown in Fig. 13.

As one can notice, the full cross-section implant made of Ti6Al4V with amplitude loading 2 kN can withstand 80 Mcycles, which is good enough for 80 years of normal activity, contrary to previous cases (1.56-5 Mcycles), obtained for different geometry, higher crack growth rate, 50 % higher amplitude loading and longer initial crack (1 vs. 0.5 mm).

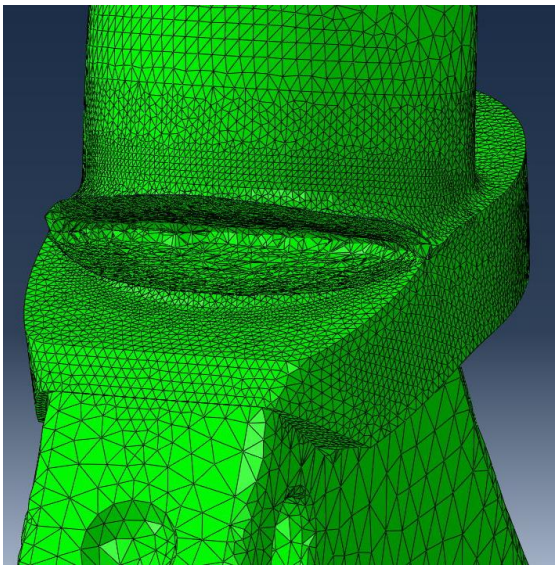

Figure 11. Crack growth over the entire length of the prosthesis.

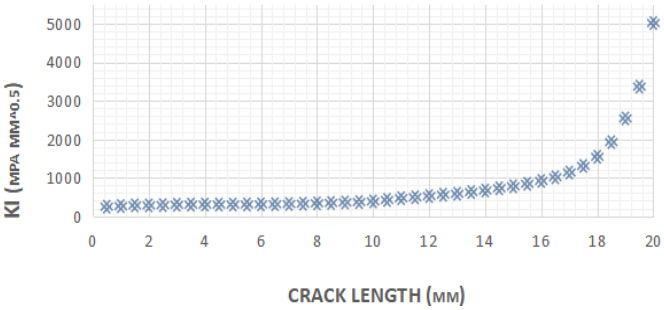

Figure 12. Change in K_I values relative to crack length.

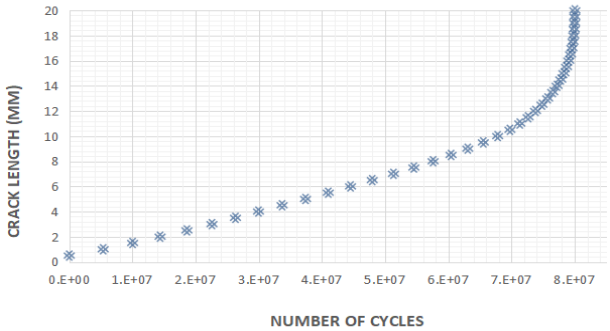

Figure 14. Crack length vs. number of walking cycles.

CASE STUDY 3 – Ti6Al4V IMPLANT WITH HOLES

In paper /25/ numerical simulation of implant for partial hip arthroplasty is performed taking into account that forces occurring in vivo can be 6-7 times the body weight. Thus, the ABAQUS finite element analysis (FEA) is performed using 3-dimensional models to evaluate stresses and strains of the femoral component at forces ranging from 2.5 (slow walk) to 6.3 kN. Hip implant with two openings, made of Ti6Al4V alloy, is analysed to estimate stress concentration in critical cross-sections of femoral component which can lead to implant fracture, as shown in Fig. 14.

Figure 14. Examples of hip implant failure.

Maximum stress values are shown in Table 3 for 4 different load cases, whereas stress distribution is shown in Fig. 15, indicating areas of maximum stresses.

Table 3. Maximum stress values.

Load case	Maximum stresses
Slow walking on a flat surface	256.3 MPa
Climbing upstairs	361.2 MPa
Tripping	535.5 MPa
Climbing downstairs	312.6 MPa

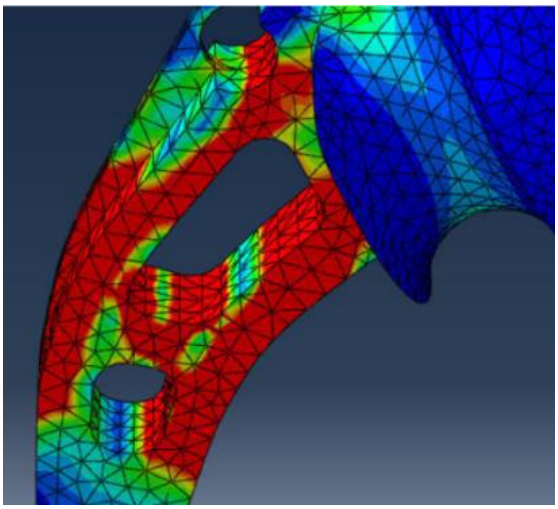

Figure 15. Results for slow walking on a flat surface.

In /26/ experimental and FEM research of mechanical behaviour of hip replacement implant is performed to verify numerical results. Experimental analysis is performed on a hip prosthesis extracted from a patient after revision surgery, Fig. 16a, by use of Digital Image Correlation (DIC) technique, Fig. 16b, whereas ABAQUS is used for numerical simulation. For the experimental measurement of strains an adapter is constructed to simulate the condition of a proximally loosened stem, Fig. 16c.

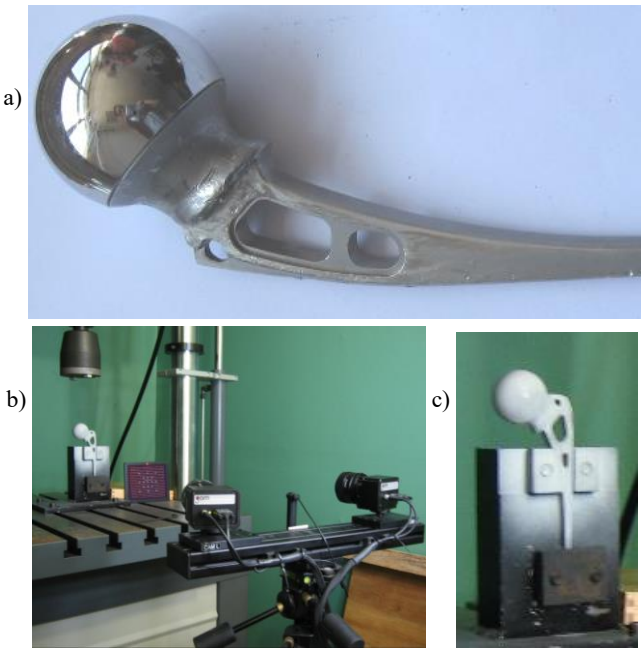

Figure 16. a) test sample; b) DIC setup; c) adapter.

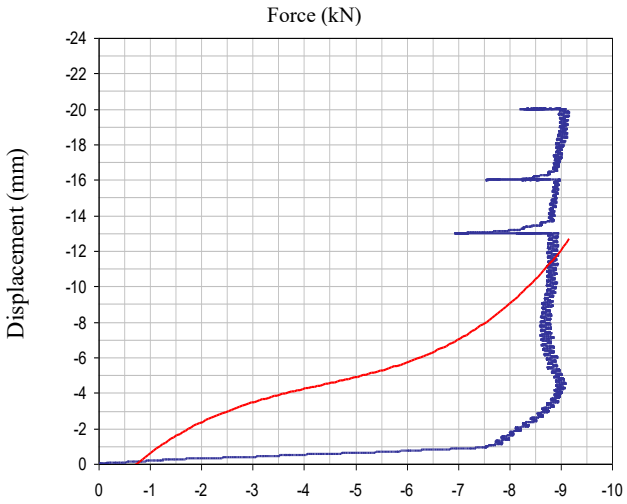

Figure 17. Diagram force-displacement for static testing.

Having in mind basic mechanical properties of Ti6Al4V alloy, yield strength 780 MPa, tensile strength 860 MPa, Young's modulus 120 GPa and Poisson ratio 0.3, /13/, one can correlate yield strength (YS) with the force 7.7 kN, Fig. 17, which represents loading at yielding initiation. Behaviour of hip implant under 6 kN force, corresponding to the worst case scenario (stumbling - tripping), is still linear elastic, according to previously mentioned YS vs. force dependence, but small plastic strain appears at point of stress concentration (e.g. force acting at single point, which is not com-

pletely realistic), as shown in Fig. 18, obtained by DIC, /26/. Final appearance of hip implant after testing is shown in Fig. 19, indicating significant plastic strains at critical point.

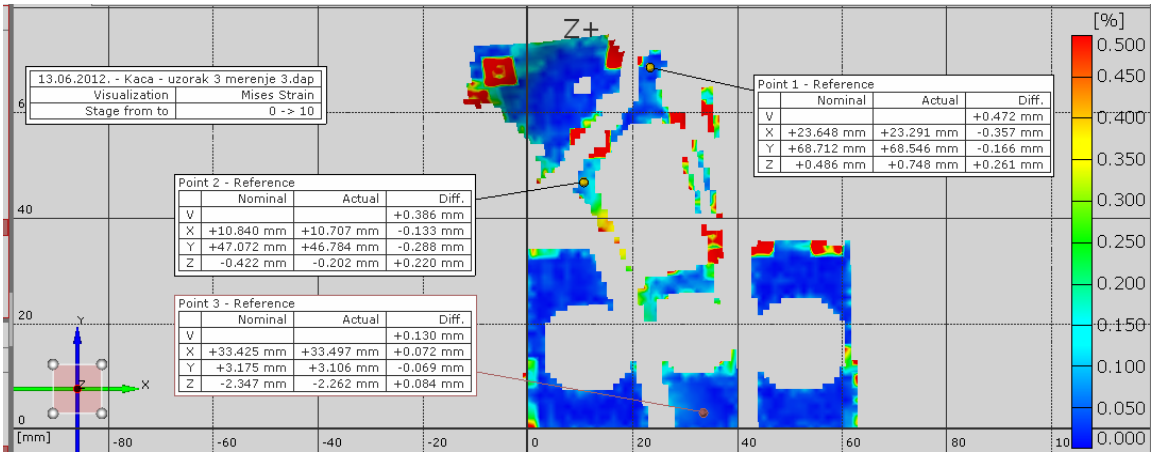

Figure 18. Strain distribution - force 6 kN /13/, 0.47 % equivalent strain, 120 GPa, corresponding stress 564 MPa.

Figure 19. Hip implant after testing.

a)

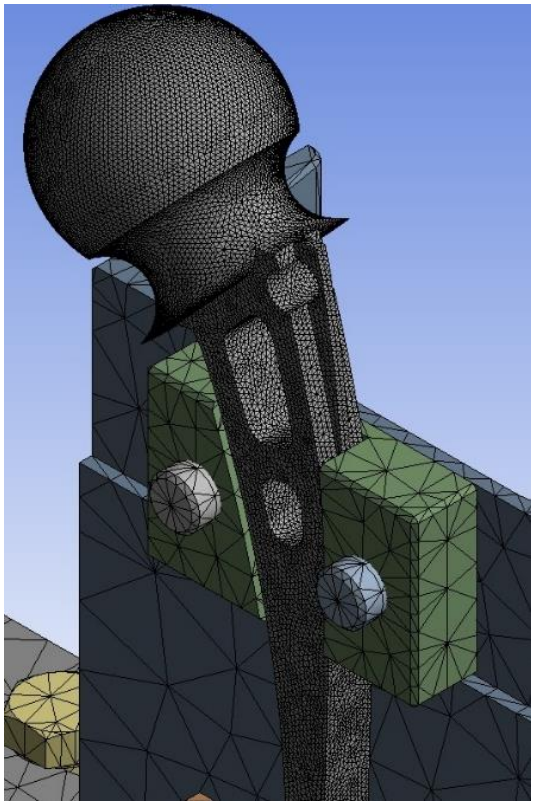

b)

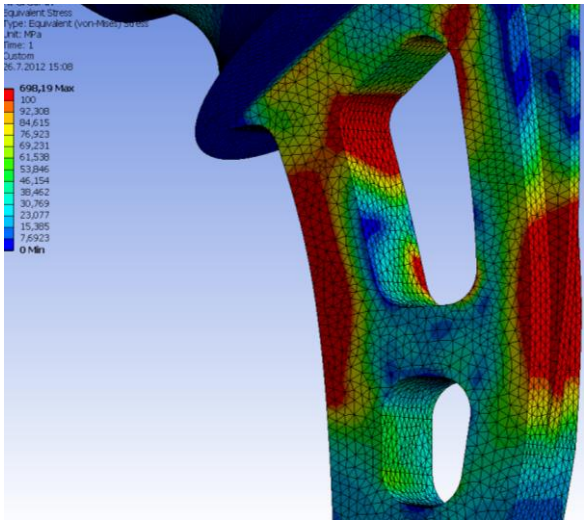

Figure 20. a) Boundary conditions of the FE model; b) stress distribution in the model.

The FE model, simulating real loading and boundary conditions as applied in the experiment, is shown in Fig. 20a, whereas Fig. 20b shows stress distribution, with maximum value 698 MPa. One should notice that stress distribution is not well presented. since the same colour is from 100 to 698 MPa. One can see that the experimental (DIC) and numerical (FEM) results are in good mutual agreement, whereas FEM results predict cca 15 % larger stresses due to concentrated force and strict boundary conditions.

In /27-29/ similar numerical analysis of stresses in partial hip implant subjected to static loads is performed. In /27/ for two different weights/forces (force 2944.8 N, weight 70 kg) and (force 5460 N, weight 130 kg). To make 3D FE models of hip implants as precise as possible 3D scanning is used in the scope of reverse engineering. Modelling is done in ANSYS, as shown in Fig. 21a-c (mesh, load and boundary conditions), providing results as shown in Fig. 21d-e for both 2944.8 N and 5460 N, indicating maximum stress values in critical areas. Furthermore, there are stresses higher than the ones picked up in Fig. 21d-e at other locations, but they are compressive stresses, and as such also dismissed from further analysis.

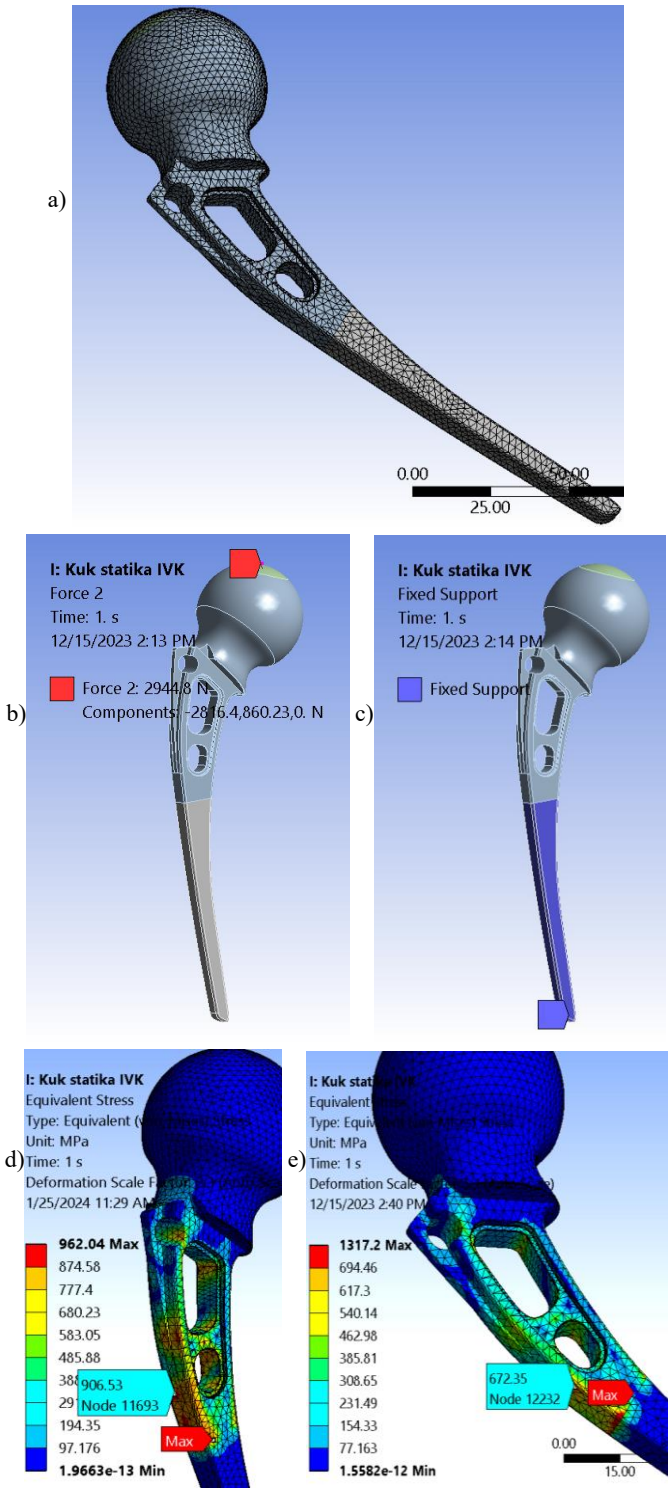

Figure 21. a) Finite element mesh; b) load defined as force; c) boundary conditions; d) stress distribution for 70 kg model; e) stress distribution for the 130 kg model.

In /28/ reverse engineering methodologies was combined with a numerical approach to analyse the structural integrity of artificial hip implants made of Ti6Al4V alloy subjected to different types of loads. In this way, numerical models validate the adopted methodology for obtaining implant geometry using 3D scanning, while also providing valuable insight into the behaviour of hip implants under different static loading cases. Since 3D scanning is proven as efficient and reliable for obtaining accurate geometry of various types of implants, it is applied in this research. Following a detailed development of a hip implant model geometry, involving 3D scanning and refining the obtained point cloud to a level that would realistically represent the actual hip implant, numerical models are made based on the obtained geometry. Results of these simulations using the finite element method in ANSYS® software have provided realistic values of stresses in most critical areas of the hip implant, Fig. 22. The precise value of load that would produce plastic strain on the implant is also determined and is used as the limit criterion for selecting load cases for further analysis. This analysis would involve the assessment of fatigue life of hip implants with the same geometry and the same material while assuming the presence of a crack in the most critical area. Obtained loads are as follows: walking 2490 N; downstairs 3143 N; upstairs 3417 N; tripping 6358 N, and results for stresses and strains are shown in Fig. 23.

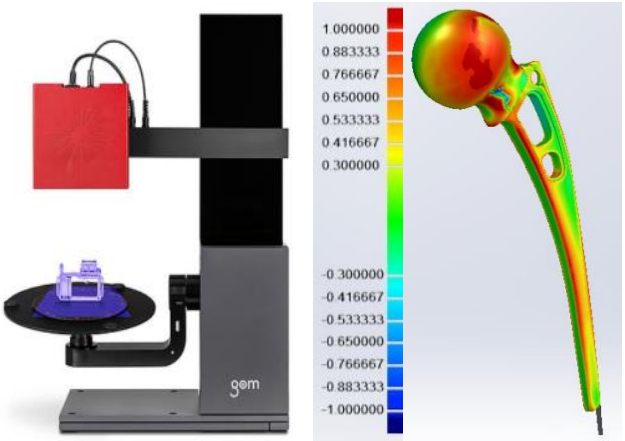

Figure 22. Atos Core 200 3D scanner setup /31/ and the deviation analysis of CAD model from dedicated mesh.

Finally, it can be seen that the results obtained by this research indicate the following: climbing stairs can cause plastic strain for the given geometry of the implant, for a body weight of 90 kg. This particular optimised hip implant geometry, which includes two holes in the stem, is not an ideal solution for selected body weight, due to plastic strain occurring even under static load. One should notice that in this case the neck is not a problem, but the holes are. One should also notice that stresses obtained for implant with two holes are very high, i.e., critical even in the case of static loading, since maximal values are close to yield strength.

In /29/ additional experimental and numerical analysis of orthopaedic implants (with two openings) with crack-type defects is performed to assess its fatigue life. Although rare, femoral component failures are well-documented complications that can occur after hip implantation. Most stem fractures happen in the first third of the implant due to the loosening of the proximal stem and fixation of the distal stem, leading to bending and eventual fatigue failure. Experimental analyses of the mechanical behaviour of implants subjected to loads according to relevant standards, using a new combined approach, including both experiments and numerical simulations is presented. The tensile properties of the titanium alloy are experimentally determined, along

with Paris law coefficients C and m, Fig. 24. The finite element software ANSYS® 2022R2 version is used to develop the three-dimensional model with a crack Fig. 25, and to calculate stresses Fig. 26a, stress intensity factors Fig. 26b, and the number of cycles Fig. 26c. The results for fatigue life of a partial hip implant subjected to various load cases, defined as load spectrum, indicate significant differences in behaviour by patient specific activities. In any case, the number of cycles for crack to grow from 0.1 mm to 2.5 mm (approximately) is several hundreds of thousands, entering critical phase of growth.

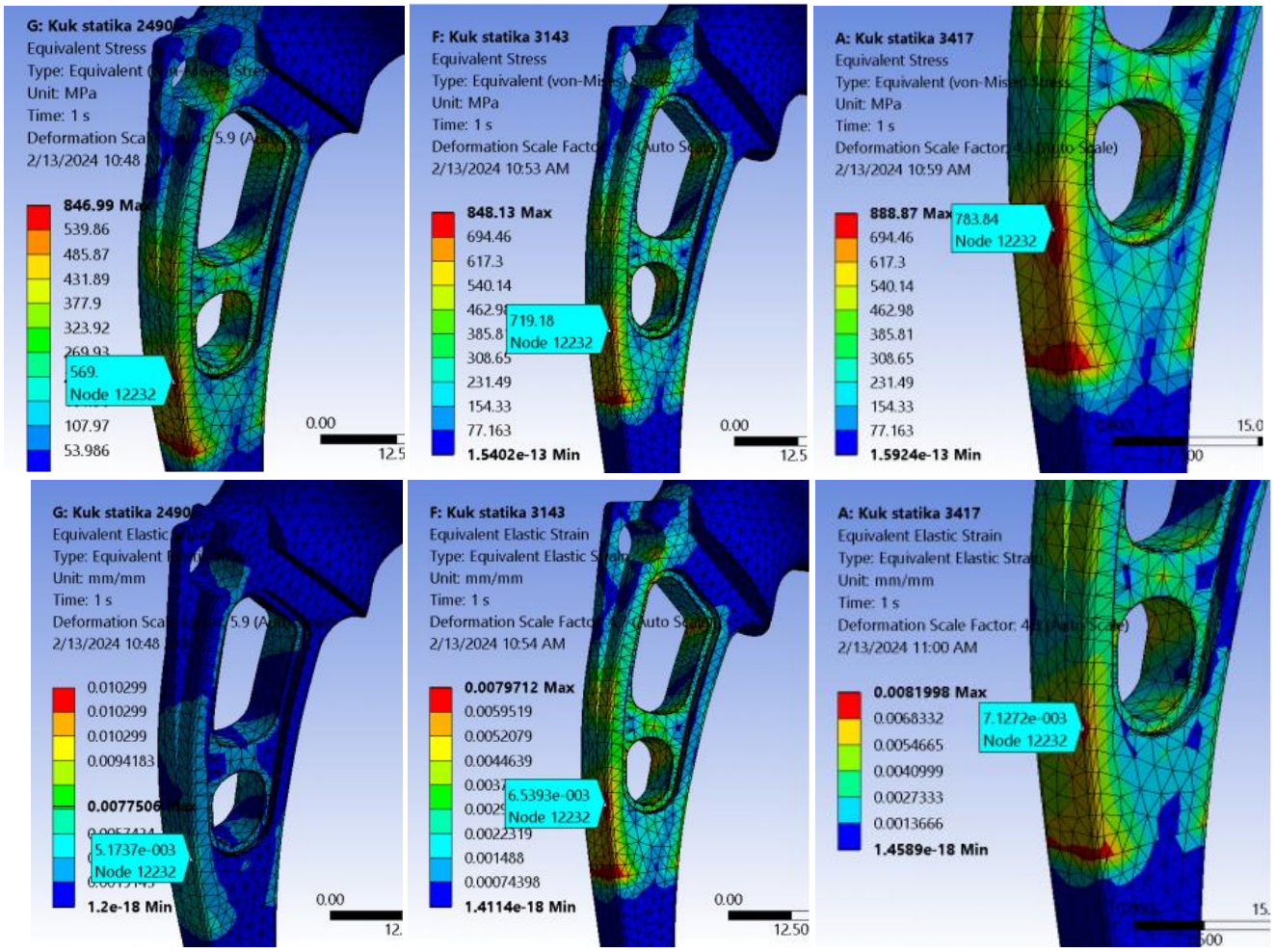

a) first load case, 2490 N force b) second load case, 3143 N force c) third load case, 3417 N force

Figure 23. Stress and strain distribution for all three load cases.

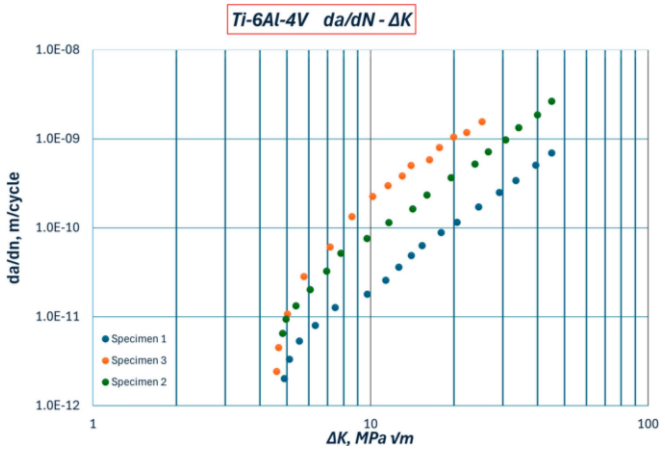

Figure 24. Experimental da/dN-ΔK curves used for obtaining the Paris coefficients C and m.

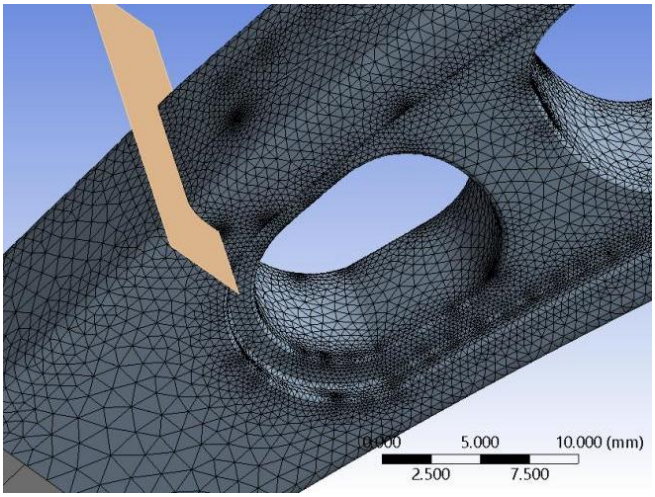

Figure 25. Initial fatigue crack and its mesh.

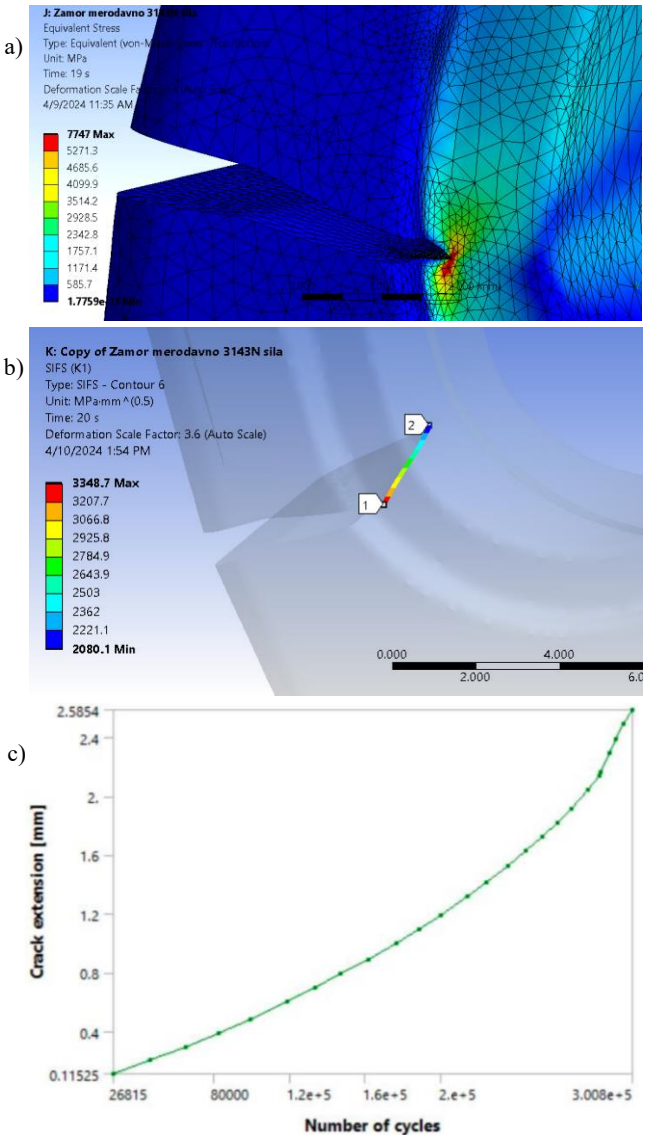

Figure 26. Results for the 3415 N force: a) stress distribution; b) stress intensity factors along crack front; c) *a*-N diagram.

Results for fatigue crack growth also indicate that the geometry with two holes is not sufficiently resistant to hip implant loading, since only 300 Kcycles is obtained for crack growth from 0.1 to 2.5 mm.

DISCUSSION AND CONCLUSIONS

Case studies 1 to 3 are presented here with an aim to compare different hip implant materials and geometries.

Comparison of CoCr and Ti6Al4V alloys reveals a bit surprising difference in favour to the later, especially regarding better resistance to fatigue crack growth. Keeping in mind significantly smaller E (approximately 2 times) and thus smaller shielding effect, Ti6Al4V alloy seems to be a better option. For the more comprehensive comparison, the environmental effects should be also taken into account, as it will be shown in the future paper.

Comparison of geometry with full cross-section vs. the geometry with two holes reveals high crack sensitivity of the later, even to static loading, and especially to the fatigue life, so their advantages (smaller mass, easier manipulation during surgery) are generally not as strong as their disadvantages. If one still would prefer geometry with two holes, the holes should be as small as possible.

Anyhow, one should keep in mind that maximal stresses are obtained close to fixed points, which is not completely realistic, since some movement of implant is possible due to flexibility of cement used for fixing. This issue should be further investigated with more realistic boundary conditions.

Finally, representing load as a concentrated force causes significant plastic strain in non-realistic locations, namely the implant head, and future models should consider the possibility of defining a load in distributed form over a small part of the implant head surface.

REFERENCES

1. Bäcker, H.C., Wu, C.H., Kienzle, A., et al. (2023), *Mechanical failure of total hip arthroplasties and associated risk factors*, Arch. Orthop. Trauma Surg. 143(2): 1061-1069. doi: 10.1007/s00402-022-04353-0
2. Wilson, D.A., Dunbar, M.J., Amirault, J.D., Farhat, Z. (2010), *Early failure of a modular femoral neck total hip arthroplasty component: A case report*, J Bone Jt. Surg. 92(6): 1514-1517. doi: 10.2106/JBJS.I.01107
3. Murena, L., Maritan, G., Concina, C., et al. (2019), *Fracture of cobalt-crome modular neck in total hip arthroplasty*, Acta Biomed. 90(12-S): 187-191. doi: 10.23750/abm.v90i12-S.8941
4. Kovač, S., Mavčič, B., Kotnik, M., et al. (2019), *What factors are associated with neck fracture in one commonly used bimodular THA design? A multicenter, nationwide study in Slovenia*, Clin. Orthop. Relat. Res. 477(6): 1324-1332. doi: 10.1097/CORR.0000000000000646
5. Krueger, D.R., Guenther, K.-P., Deml, M.C., Perka, C. (2020), *Mechanical failure of 113 uncemented modular revision femoral components*, Bone Joint J, 102-B(5): 573-579. doi: 10.1302/0301-620X.102B5.BJJ-2019-1333.R2
6. Hernandez-Rodriguez, M.A.L., Ortega-Saenz, J.A., Contreras-Hernandez, G.R. (2010), *Failure analysis of a total hip prosthesis implanted in active patient*. J Mech. Behav. Biomed. Mater. 3(8): 619-622. doi: 10.1016/j.jmbbm.2010.06.004
7. Kobayashi, N., Yukizawa, Y. (2023), *Causes of failure after total hip arthroplasty: A narrative review of literatures*, J Jt. Surg. Res. 1(1): 56-61. doi: 10.1016/j.jjoisr.2023.01.006
8. Jamari, J., Ammarullah, M.I., Santoso, G., et al. (2022), *In silico contact pressure of metal-on-metal total hip implant with different materials subjected to gait loading*, Metals, 12(8): 1241. doi: 10.3390/met12081241
9. Yang, D.T., Zhang, D., Arola, D.D. (2010), *Fatigue of the bone/cement interface and loosening of total joint replacements*, Int. J Fatigue, 32(10): 1639-1649. doi: 10.1016/j.ijfatigue.2010.03.005
10. Dall'Ava, L., Hothi, H., Di Laura, A., et al. (2019), *3D printed acetabular cups for total hip arthroplasty: a review article*, Metals, 9(7): 729. doi: 10.3390/met9070729
11. Griza, S., dos Santos, S.V., Ueki, M.M., et al. (2013), *Case study and analysis of a fatigue failure in a THA stem*, Eng. Fail. Anal. 28: 166-175. doi: 10.1016/j.engfailanal.2012.10.011
12. Zajc, J., Moličnik, A., Fokter, S.K. (2021), *Dual modular titanium alloy femoral stem failure mechanisms and suggested clinical approaches*, Materials, 14(11): 3078. doi: 10.3390/ma14113078
13. Norman, P., Iyengar, S., Svensson, I., Flivik, G. (2014), *Fatigue fracture in dual modular revision total hip arthroplasty stems: failure analysis and computed tomography diagnostics in two cases*, J Arthroplasty, 29(4): 850-855. doi: 10.1016/j.arth.2013.09.008

14. Corda, J.V., Chethan, K.N., Shenoy, S.B., et al. (2023), *Fatigue life evaluation of different hip implant designs using finite element analysis*, J Appl. Eng. Sci. 21(3): 896-907. doi: 10.5937/jaes0-44094
15. Beaulé, P.E., Lee, J.L., Le Duff, M.J., et al. (2004), *Orientation of the femoral component in surface arthroplasty of the hip. A biomechanical and clinical analysis*, J Bone Jt. Surg. Am. 86 (9): 2015-2021. doi: 10.2106/00004623-200409000-00021
16. Taylor, D. (2018), *Observations on the role of fracture mechanics in biology and medicine*, Eng. Fract. Mech. 187: 422-430. doi: 10.1016/j.engfracmech.2018.01.002
17. Legweel, K.M.B., *Effect of biomaterial on integrity and life of artificial hip*, Doctoral thesis, University of Belgrade, Faculty of Mechanical Engineering, 2016.
18. Čolić, K., Grbović, A., Sedmak, A., Legweel, K. (2019), *Application of numerical methods in design and analysis of orthopedic implant integrity*, In: Mitrović, N., Milošević, M., Mladenović, G. (Eds.) Experimental and Numerical Investigations in Material Science and Engineering, CNNTech 2018, Lecture Notes in Networks and Systems, vol.54. Springer, Cham. pp.96-111. doi: 10.1007/978-3-319-99620-2_8
19. Mijatović, T., Milovanović, A., Sedmak, A., et al. (2019), *Integrity assessment of reverse engineered Ti-6Al-4V ELI total hip replacement implant*, Struct. Integr. Life, 19(3): 237-242.
20. Milovanović, A., Sedmak, A., Grbović, A., et al. (2020), *Design aspects of hip implant made of Ti-6Al-4V extra low interstitials alloy*, Procedia Struct. Integr. 26: 299-305. doi: 10.1016/j.prostr.2020.06.038
21. Smoljanić, T., Milovanović, A., Sedmak, S., et al. (2023), *Numerical simulation of titanium alloy hip replacement implants behaviour under static and dynamic loads*, Hemijska Industrija, 77(4): 283-292. doi: 10.2298/HEMIND22 1118026S
22. Sedmak, A., Čolić, K., Grbović, A., et al. (2019), *Numerical analysis of fatigue crack growth of hip implant*, Eng. Fract. Mech. 216: 106492. doi: 10.1016/j.engfracmech.2019.106492
23. Smoljanić, T., et al. (2024), *Numerical investigation of fatigue behavior in Ti-6Al-4V orthopedic hip implants subjected to different environments*, Materials, 17(15): 3796. doi: 10.3390/ma17153796
24. Smoljanić, T., Sedmak, S., Sedmak, A., et al. (2022), *Experimental and numerical investigation of Ti-6Al-4V alloy behaviour under different exploitation conditions*, Struct. Integr. Life, 22 (3): 353-357.
25. Čolić, K., Sedmak, A., Grbović, A., et al. (2016), *Finite element modeling of hip implant static loading*, Procedia Eng. 149: 257-262. doi: 10.1016/j.proeng.2016.06.664
26. Čolić, K., Sedmak, A., Legweel, K., et al. (2017), *Experimental and numerical research of mechanical behaviour of titanium alloy hip implant*, Tech. Gazzete, 24(3): 709-713. doi: 10.17559/TV-20160219132016
27. Čolić, K., Sedmak, S., Sedmak, A., et al. (2024), *Numerical analysis of static stresses in partial hip implant*, Struct. Integr. Life, 24(1): 17-20. doi: 10.69644/ivk-2024-01-0017
28. Čolić, K., Sedmak, S., Dascau, A.A., et al. (2024), *Reverse engineering and finite element analysis of Ti-6Al-4V orthopaedic HIP implants*, Struct. Integr. Life, 24(3): 269-275. doi: 10.69644/ivk-2024-03-0269
29. Čolić, K., Kostić, S.M., Sedmak, S., et al. (2025), *Structural integrity and life assessment of Ti-6Al-4V orthopaedic implants*, Metals, 15(3): 333. doi: 10.3390/met15030333
30. Sedmak, A. (2024), *Fatigue crack growth simulation by extended finite element method: A review of case studies*, Fatigue Fract. Eng. Mater. Struct. 47(6): 1819-1855. doi: 10.1111/ffe.14277
31. Sedmak, A. (2018), *Computational fracture mechanics: An overview from early efforts to recent achievements*, Fatigue Fract. Eng. Mater. Struct. 41(12): 2438-2474, doi: 10.1111/ffe.12912
32. Sedmak, A., Grbović, A., Sedmak, S. (2025), *Structural integrity and life assessment of railway and aeronautical components - Review of four case studies*, Theor. Appl. Fract. Mech. 139(Part A): 105008. doi: 10.1016/j.tafmec.2025.105008